J. Biochem. 2009;145(2)161–168
doi:10.1093/jb/mvn152

Prostaglandin $F_{2\alpha}$ Synthase Activities of Aldo–Keto Reductase 1B1, 1B3 and 1B7

Zakayi Kabututu[1], Michèle Manin[2], Jean-Christophe Pointud[2], Toshihiko Maruyama[1], Nanae Nagata[1], Sarah Lambert[2], Anne-Marie Lefrançois-Martinez[2], Antoine Martinez[2] and Yoshihiro Urade[1,*]

[1]Department of Molecular Behavioral Biology, Osaka Bioscience Institute, 6-2-4 Furuedai, Suita, Osaka 565-0874, Japan; and [2]CNRS, UMR6247—Genetic, Reproduction and Development (GReD), Clermont University, 63177 Aubière, France

Received September 4, 2008; accepted October 30, 2008; published online November 14, 2008

Here, we show that three enzymes belonging to the 1B group of the aldo–keto reductase (AKR) superfamily, i.e., human placental aldose reductase (AKR1B1), mouse kidney aldose reductase (AKR1B3) and mouse vas deferens protein (AKR1B7), catalyse the reduction of prostaglandin (PG) H_2, a common intermediate of various prostanoids, to form $PGF_{2\alpha}$ in the presence of NADPH. AKR1B1, AKR1B3 and AKR1B7 displayed higher affinities for PGH_2 (K_m = 1.9, 9.3 and 3.8 μM, respectively) and V_{max} values (26, 53 and 44 nmol/min/mg protein, respectively) than did the human lung $PGF_{2\alpha}$ synthase (AKR1C3; 18 μM and 4 nmol/min/mg protein, respectively). The $PGF_{2\alpha}$ synthase activity of AKR1B1 and AKR1B3 was efficiently inhibited by two AKR inhibitors, tolrestat (K_i = 3.6 and 0.26 μM, respectively) and sorbinil (K_i = 21.7 and 0.89 μM, respectively), in a non-competitive or mixed-type manner, whereas that of AKR1B7 was not sensitive to these inhibitors (K_i = 9.2 and 18 mM, respectively). These data provide a molecular basis for investigating novel functional roles for AKR1B members and $PGF_{2\alpha}$ as mediators of physiological and pathological processes in mammalian organisms.

Key words: prostaglandin $F_{2\alpha}$, prostaglandin H_2, prostaglandin H_2 $F_{2\alpha}$-reductase, tolrestat, sorbinil.

Abbreviations: AKR, aldo–keto reductase; ARI, aldose reductase inhibitors; ARLP, aldose reductase-like proteins; LC–MS, liquid chromatography–mass spectrometry; PG, prostaglandin; PGFS, prostaglandin $F_{2\alpha}$ synthase.

INTRODUCTION

Prostaglandin (PG) $F_{2\alpha}$ is actively produced in many tissues of mammals and plays various important biological roles such as the contraction of uterine, bronchial, vascular and arterial smooth muscle; regulation of intraocular pressure, renal filtration and ovarian cycle through induction of luteolysis; inhibition of adipose differentiation (*1*); and stimulation of hair growth (*2*). However, the mechanism for the production of $PGF_{2\alpha}$ is not clearly understood. Three different pathways have been reported in terms of $PGF_{2\alpha}$ production (*3*), i.e., 9,11-endoperoxide reduction of PGH_2, 9-ketoreduction of PGE_2 and 11-ketoreduction of PGD_2 (Fig. 1); although the last results in the production of 9α,11β-PGF_2, a stereo-isomer of $PGF_{2\alpha}$.

The conversion of the 9,11-endoperoxide group of PGH_2 to 9- and 11-hydroxy groups of $PGF_{2\alpha}$ is catalysed by PGF synthase (PGFS). Most known PGFSs belong to the aldo–keto reductase (AKR) superfamily (*3*), which comprises monomeric proteins that bind nicotinamide cofactors. AKR proteins are widely distributed in mammals, amphibians, plants, yeast, protozoa and bacteria and metabolize a number of substrates including aldehydes, monosaccharides, steroids, polycyclic hydrocarbons, isoflavonoids and PGs (*4*). To date, PGFS activity has been demonstrated for various AKR members. In mammals, AKR1C subfamily enzymes with PGFS activity (EC 1.1.1.188) were isolated from bovine liver (*5*, *6*) and lung (*6*) as well as human lung (*7*). Protozoan enzymes designated as AKR5A2 and AKR5A1 (EC 1.1.1.188) were isolated from *Trypanosoma brucei* (*8*) and the old-world species of *Leishmania* (*9*), respectively.

Aldose reductase (EC 1.1.1.21), the prototype of AKR1B subfamily, named AKR1B1 in human and AKR1B3 in mouse, is the first and rate-limiting enzyme of the polyol pathway that reduces glucose to sorbitol and contributes to secondary diabetic complications (*10*). In addition, AKR1B subfamily enzymes catalyse the reduction of toxic aldehydes generated by several metabolic pathways including lipid peroxidation and steroidogenesis with much better efficiency than the reduction of glucose, supporting the view that they are components of a cellular antioxidant defence mechanism (*11*, *12*). However, recent evidences suggest that members of the AKR1B subfamily may also be endowed with PGFS activity. Indeed, the bovine aldose reductase, AKR1B5, was shown to cumulate both 20α-hydroxysteroid dehydrogenase activity and catalytic ability to produce $PGF_{2\alpha}$ in the endometrium (*13*). Beside the canonical aldose

*To whom correspondence should be addressed. Tel: +81-6-6872-4851, Fax: +81-6-6872-2841, E-mail: uradey@obi.or.jp

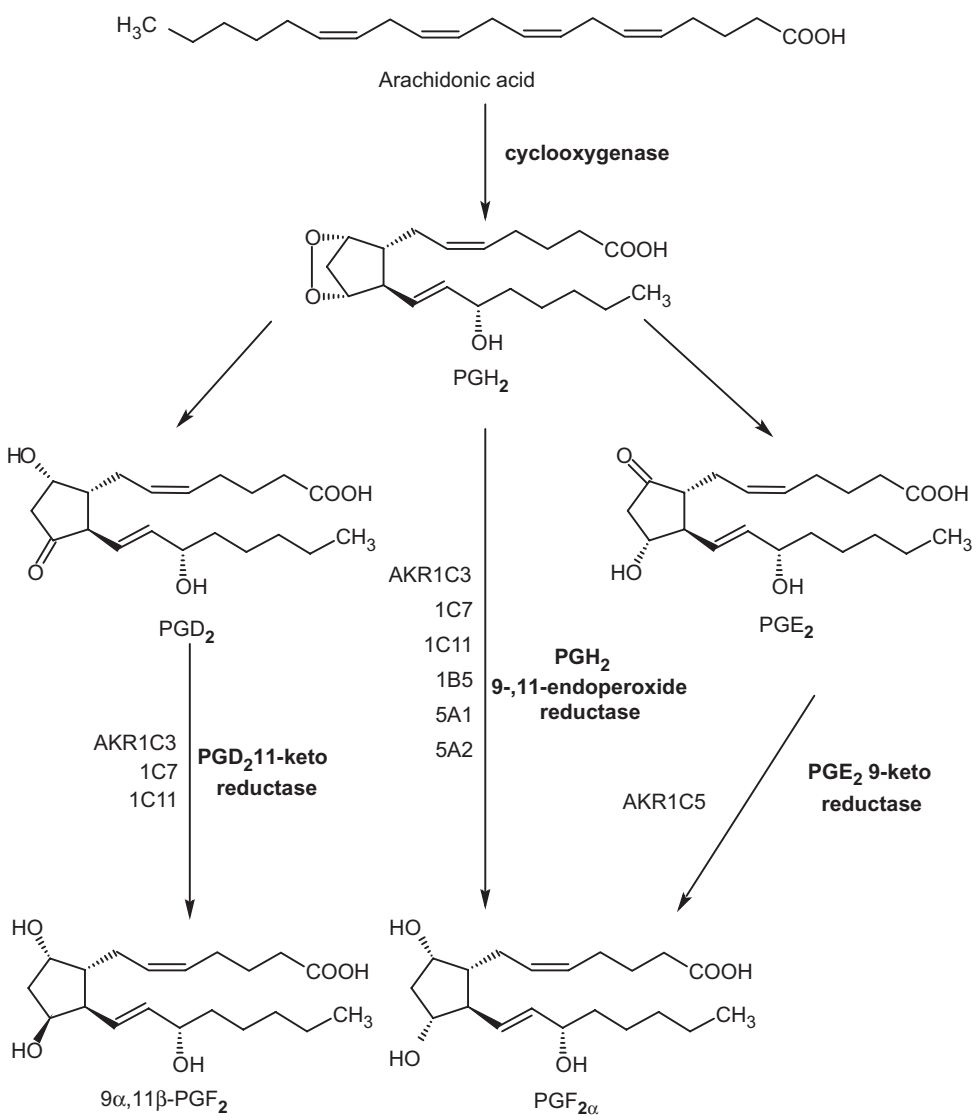

Fig. 1. **$PGF_{2\alpha}$ biosynthetic pathways.** The members of AKR family catalyzing each reaction are also presented.

reductases with ubiquitous expressions (AKR1B1, AKR1B3, AKR1B5), a second group named aldose reductase-like proteins (ARLP) have been characterized on the basis of sequence homology (at least 60–70% identity with aldose reductase). Several ARLP with both a poor efficiency in reducing glucose and a more tissue-restricted expression have been identified in mouse, AKR1B7 (*14–16*), AKR1B8 (*17*) and in human, AKR1B10 (*18*, *19*).

The well-characterized human lung PGFS also named AKR1C3 is used as the reference PGFS enzyme in the current study and is a member of AKR1C subfamily, which comprises proteins with a hydroxysteroid dehydrogenase activity. The human PGFS catalyses the reduction of PGH_2 and PGD_2 into $PGF_{2\alpha}$ and 9α,11β-PGF_2, respectively, but does not use PGE_2 as substrate (*7*). Crystallographic studies of AKR1C3 and isoforms AKR1C1 and AKR1C2 indicate broader substrate specificity for AKR1C3 in comparison with other members of AKR1C subfamily (*20*).

In this study, we examined whether five members of AKR1B subfamily from human and mouse produced $PGF_{2\alpha}$ from PGH_2 and found that AKR1B1, AKR1B3 and AKR1B7 are more efficient PGFS than AKR1C3.

EXPERIMENTAL PROCEDURES

Expression and Purification of Recombinant AKR Enzymes—Open reading frames of AKR1B1, AKR1B3, AKR1B7, AKR1B8 and AKR1B10 were inserted between *Nde*I and *Bam*HI/*Eco*RI sites of the expression vector pET-28a as described previously (*21*, *22*) and used for transformation of *Escherichia coli* BL21DE3. The outside primers used for PCR amplifications of inserts were as follows: 5′ B1 *Nde*I primer (5′-CGGCAG*CCATAT*GGCA AGCCGTC-3′) and 3′ B1 *Eco*RI primer (5′-CG*GAATTC* GGGCTTCAAAACTCTTCATGG-3′); 5′ B3 *Nde*I primer (5′-CGGCAG*CCATAT*GGCCAGCCATC-3′) and 3′ B3 *Eco*RI primer (5′-CAC*GAATTC*CAGAGAGACACAGGA

CACTTGC-3′); 5′ B7 *Nde*I primer (5′-CGGCAG*CCATAT* GGCCACCTTCGT-3′) and 3′ B7 *Bam*HI primer (5′-CG *GGATCC*CGTCAGTATTCCTCGTGG-3′); 5′ B8 *Nde*I primer (5′-CGGCAG*CCATAT*GGCCACGTTCGTGG-3′); 3′ B8 *Bam*HI primer (5′-CG*GGATCC*CGGGGCTGA CTCAGCTTCA-3′); 5′ B10 *Nde*I primer (5′-CGGCA G*CCATAT*GGCCACGTTTGTGG-3′) and 3′ B10 *Bam*HI primer (5′-TAAC*GGATCC*ACCAGGAGATTCAACC-3′). Transformed cells were precultured overnight at 30°C. Induction was started by the addition of 1 mM isopropyl-β-D-thiogalactopyranoside once the optical density value at 600 nm of the cultures had reached 0.5–0.6. The cultures were maintained at 30°C for 5 h and then harvested and disrupted by sonication (10 bursts of 10 s each with 10 s interval on an ice bath). The resulting supernatant of recombinant proteins was purified by chromatography with Ni-NTA His-Bind resin (Novagen) according to the manufacturer's protocol and cleaved from His tag with thrombin (10 U/mg of fusion protein). The recombinant proteins were then loaded onto a gel filtration Hiload 16/60 Superdex 200 pg column (Amersham Biosciences) and eluted with phosphate-buffered saline at a flow rate of 1 ml/min. AKR1C3 was purchased from Cayman Chemical (Ann Arbor, MI). Protein purity was assessed by SDS–PAGE on 12.5% gels after staining with Coomassie Brilliant Blue. Protein concentration was determined by bicinchinonic acid protein assay (Pierce) according to the manufacturer's protocol.

Enzyme Assays—The PGFS activity was determined as described previously (*8*). In brief, the purified enzymes (20 μg) were incubated at 37°C for 2 min with 10 μM [1-^{14}C] PGH_2 in the presence of 500 μM NADPH in 50 mM sodium phosphate, pH 7.0. The reaction was stopped by the addition of 300 μl of diethyl ether/methanol/2 M citric acid (30:4:1 vol/vol/vol). The PG products were extracted and separated by thin-layer chromatography (TLC) as follows. The PG extracts were applied to 20 cm × 20 cm silica gel plates (Merck KGaA) at 4°C, and the plates were developed in a solvent system consisting of 90:2:1 vol/vol/vol diethyl ether/methanol/acetic acid at −20°C. The radioactivity on the plates was analysed by Fluorescent Imaging Analyser FLA 2000 and Mac Bas V2.5 software (Fuji Photo Film Co.).

PGD_2 11-ketoreductase and PGE_2 9-ketoreductase activities were determined with 500 μM NADPH and 10 μM [1-^{14}C] PGD_2 or PGE_2, which was prepared from [1-^{14}C] PGH_2 by incubation with hematopoietic PGD synthase or microsomal PGE synthase-1, respectively, as described previously (*8*).

p-Nitrobenzaldehyde reductase activity of AKR1B enzymes was determined spectrophotometrically (*8*). For enzyme inhibition assays, AKR1B enzymes were incubated with various concentrations of tolrestat or sorbinil.

Liquid Chromatography–Mass Spectrometry (LC–MS) Analysis—LC–MS analyses of $PGF_{2\alpha}$ were performed by using a Waters Associates (Milford) HPLC–MS system equipped with a 2,695 separation module, a 996 photodiode array detector and ZQ-4000 mass spectrometry detector with electron spray ionization source. $PGF_{2\alpha}$ was generated as described earlier by incubating 100 μg of PGH_2 (Cayman Chemical) with 200 μg recombinant AKR1B proteins, and the product was extracted, dried and resuspended in 100 μl of ethanol. For chromatographic separation, $PGF_{2\alpha}$ products or authentic PGs were run on an Inertsil ODS-3, 5 μm, 250 × 2.1-mm column (GL Sciences Inc) using a 37–80% v/v acetonitrile gradient (in 0.02% v/v formic acid) at a flow rate of 0.2 ml/min over 20 min with the column temperature set at 37°C. For mass spectrometric conditions, the electron spray ionization interface was operated at a source temperature of 115°C and a desolvation temperature 350°C. Cone gas and desolvation gas flow were 124 and 606 l/h, respectively. Cone voltage for each PG was followed. Authentic $PGF_{2\alpha}$, 9β,11α-PGF_2, 8-iso $PGF_{2\alpha}$ and 9α,11β-PGF_2 used as standards in LC–MS analysis were obtained from Cayman Chemical.

RESULTS

Formation of $PGF_{2\alpha}$ from PGH_2 by AKR1B Enzymes—Recombinant AKR1B1, AKR1B3, AKR1B7, AKR1B8 and AKR1B10 were expressed in *E. coli* as fusion proteins, cleaved with thrombin to remove the 6xHis-tag and purified to apparent homogeneity. The purified proteins migrated as single bands of similar mobility on SDS–PAGE indicating a molecular mass of about 35,000 (Fig. 2A). This mass is in agreement with the calculated molecular masses of 35,722; 35,615; 35,844; 35,989; and 35,890 for AKR1B1, AKR1B3, AKR1B7, AKR1B8 and AKR1B10, respectively, and smaller than that of human $PGF_{2\alpha}$ synthase AKR1C3, which is 36,842 (*7*).

We incubated these AKR proteins with 10 μM [1-^{14}C] PGH_2 in the presence of 0.5 mM NADPH and analysed the reaction products by TLC (Fig. 2B). AKR1B1, AKR1B3 and AKR1B7 reduced the 9,11-endoperoxide group of PGH_2 to produce $PGF_{2\alpha}$. On the other hand, AKR1B8 and AKR1B10 displayed a weak and an unstable PGFS activity although both proteins potently catalysed the reduction of *p*-nitrobenzaldehyde (data not shown). Heat treatment of AKR1B1, AKR1B3 and AKR1B7 at 100°C for 5 min completely inactivated their PGFS activity, which was strictly dependent on the presence of NADPH. As opposed to previously reported AKR1B7 activities, e.g., isocaproaldehyde reductase and 4-hydroxynonenal reductase activities, which were preferentially NADH dependent (*21*), the PGFS activity of AKR1B7 was strictly dependent on NADPH.

When AKR1B1 was incubated with 10 μM [1-^{14}C] PGH_2, PGD_2 or PGE_2 in the presence of 0.5 mM NADPH, this enzyme catalysed only the conversion of PGH_2 to $PGF_{2\alpha}$, but neither PGD_2 to 9α,11β-PGF_2 nor PGE_2 to $PGF_{2\alpha}$, indicating that these enzymes were free from activities involving the reduction of PGD_2 or PGE_2 into $PGF_{2\alpha}$ (Fig. 2C), and thus differed from members of the 1C subfamily of AKR (*7*). Similar results were obtained when AKR1B3 or AKR1B7 was used as an enzyme in these reactions (data not shown).

LC–MS analysis (Fig. 3) revealed that the product of catalytic activity of AKR1B1 towards PGH_2 eluted at the same position as that of $PGF_{2\alpha}$ (elution time = 11.4 min in Fig. 3, left column) and differed from those of 9β,11α-PGF_2 (10.3 min), 8-iso $PGF_{2\alpha}$ (9.7 min) or 9α,11β-PGF_2 (9.2 min). Peaks corresponding to PGD_2 and PGE_2 were

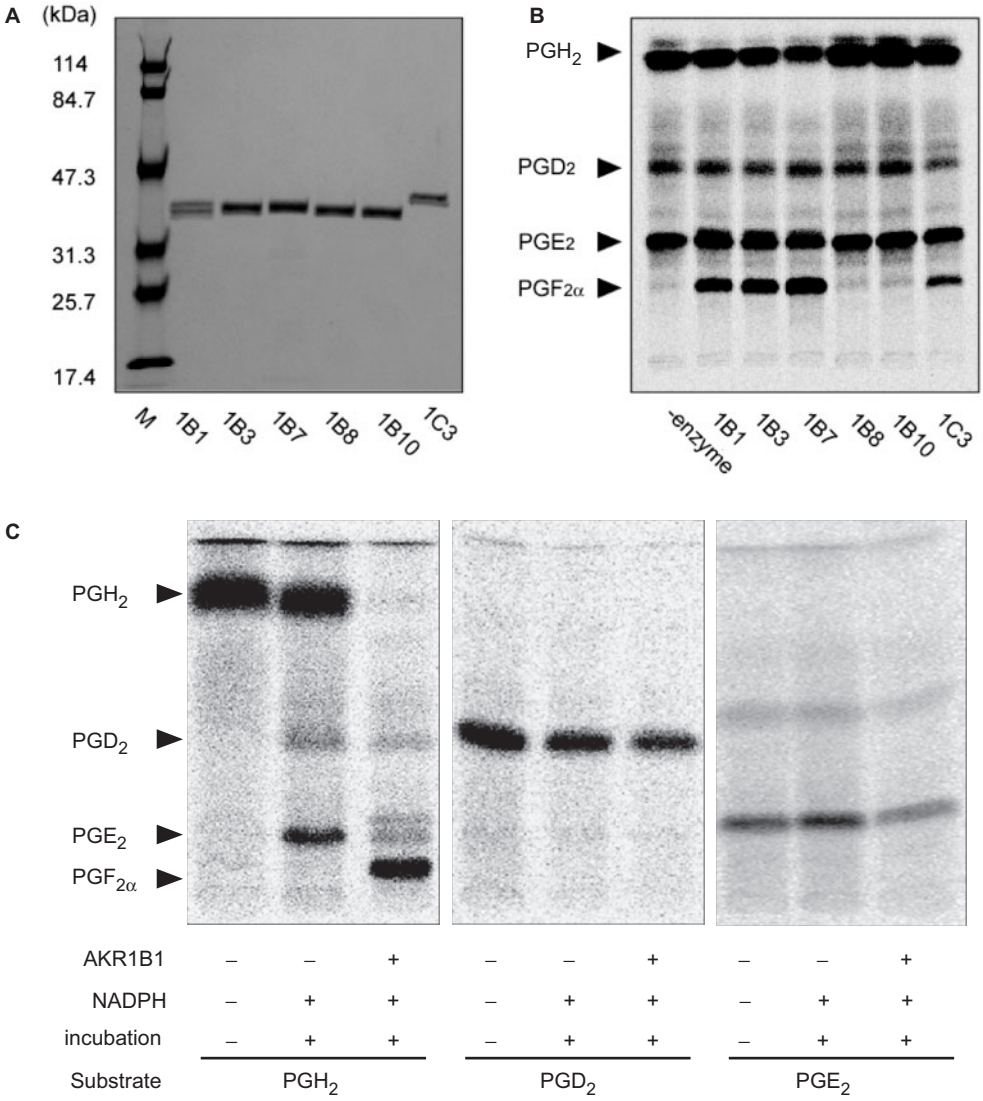

Fig. 2. **PGFS activity of recombinant AKR1B proteins.** (A) SDS–PAGE of purified recombinant AKR1B1, AKR1B3, AKR1B7, AKR1B8, AKR1B10 and AKR1C3; M, molecular mass marker proteins. (B) Autoradiogram of TLC after incubation of AKR1B proteins (each 20 μg) with 10 μM 1-[^{14}C] PGH_2 in the presence of 0.5 mM NADPH at 37°C for 2 min. (C) Autoradiogram of TLC after incubation of 10 μM 1-[^{14}C] PGH_2 (left), PGD_2 (centre) and PGE_2 (right) with 0.5 mM NADPH in the presence and absence of 100 μg of AKR1B1.

produced in absence of the enzyme (Fig. 3B), an observation that was in agreement with the non-enzymatic formation of PGD_2 and PGE_2 detected on TLC (Fig. 2B, lane-enzyme). Mass spectrometric analysis showed that AKR1B1-derived $PGF_{2\alpha}$ displayed a negative ion ($[M–H]^-$) identical to genuine $PGF_{2\alpha}$ at *m/z* 353.2 (Fig. 3C). A similar elution profile as well as mass pattern was obtained when AKR1B3 or AKR1B7 was used for the enzyme assays (data not shown). These data provide evidence that the reaction product from AKR1B-catalysed reduction of PGH_2 was indeed $PGF_{2\alpha}$.

Kinetic Parameters of AKR1B-Catalysed PGFS Activity—As summarized in Table 1, AKR1B1, AKR1B3 and AKR1B7 showed K_m values for PGH_2 of 1.9, 9.3 and 3.8 μM, respectively, which were clearly lower than the value of human PGFS classified as AKR1C3 (18 μM) and comparable with the K_m values for *p*-nitrobenzaldehyde in the AKR activities (6.4–11.6 μM). The K_m values of AKR1B1, AKR1B3 and AKR1B7 for NADPH were 5.7, 7.4 and 9.2 μM, respectively. The V_{max} values of the PGFS activity of AKR1B1, AKR1B3 and AKR1B7 (26, 53.4 and 44 nmol/min/mg protein, respectively) were 7-, 13- and 11-fold higher than that of AKR1C3 (3.9 nmol/min/mg protein). Although AKR1B1 and AKR1B3 show 5.5- and 6.5-fold higher V_{max} values of the *p*-nitrobenzaldehyde reductase activity (408.3 and 481.5 nmol/min/mg protein, respectively) than the value of AKR1C3 (74.1 nmol/min/mg), the V_{max} value of the *p*-nitrobenzaldehyde reductase activity of AKR1B7 (52.4 nmol/min/mg) was slightly lower (0.7-fold) than that of AKR1C3.

Inhibition of the PGFS Activity of AKR1B Proteins by Tolrestat and Sorbinil—We then examined the inhibitory effect of tolrestat and sorbinil, two well-studied aldose

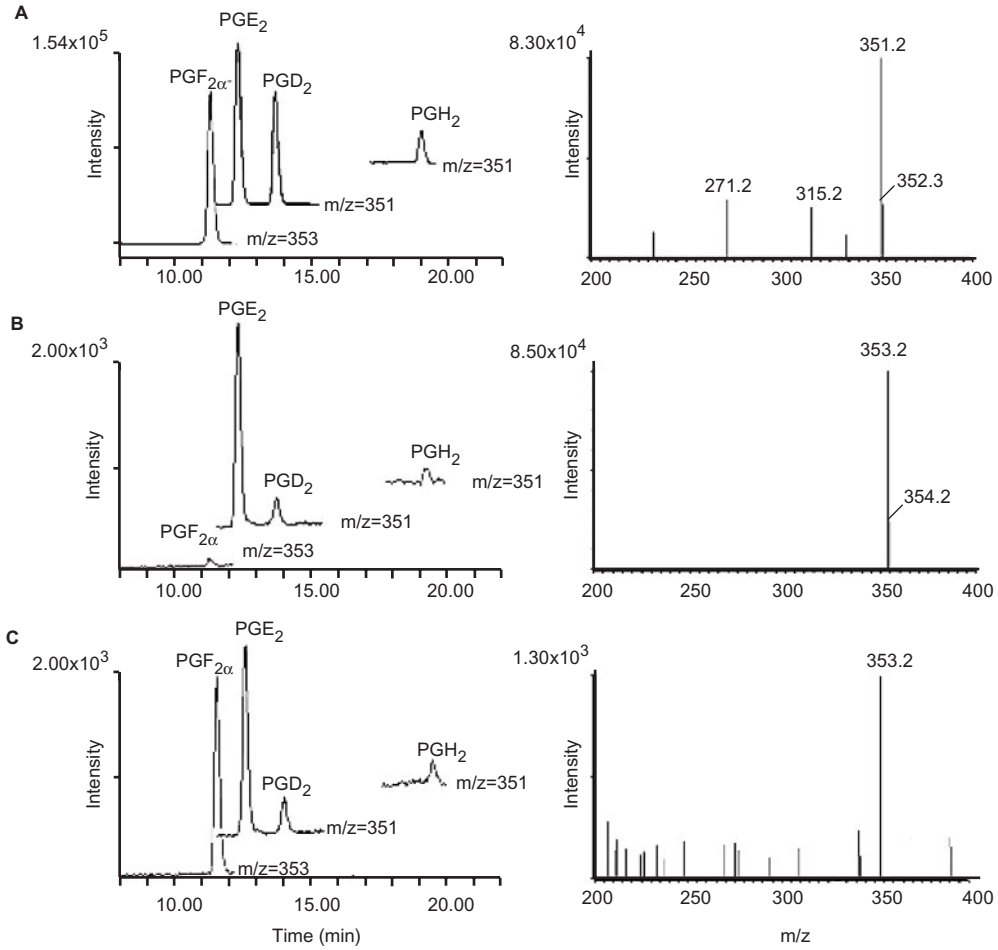

Fig. 3. **Molecular identification of AKR1B-generated $PGF_{2\alpha}$.** Elution profiles by LC (left panels) of $PGF_{2\alpha}$, PGE_2, PGD_2 and PGH_2 (A) and of the products from PGH_2 after incubation without (B) and with (C) AKR1B1. Mass spectra of the $[MH]^-$ ions (right panels) of PGH_2 (A), $PGF_{2\alpha}$ (B) and AKR1B1-produced $PGF_{2\alpha}$ (C).

Table 1. **Kinetic parameters of PGFS and AKR activities catalysed by members of the AKR superfamily.**

Enzyme	PGFS activity			Inhibition of PGFS activity		AKR activity		Inhibition of AKR activity	
	PGH_2		NADPH	PGH_2		*p*-Nitrobenzaldehyde		*p*-Nitrobenzaldehyde	
	K_m (μM)	V_{max} (nmol/min/mg)	K_m (μM)	Tolrestat K_i (μM)	Sorbinil K_i (μM)	K_m (μM)	V_{max} (nmol/min/mg)	Tolrestat K_i (nM)	Sorbinil K_i (nM)
AKR1B1	1.9 ± 1.5	26.0 ± 6.2	5.7 ± 0.7	3.6 ± 0.5	21.7 ± 14.0	11.6 ± 2.1	408.3 ± 12.7	46.1 ± 7.3	116.6 ± 12.3
AKR1B3	9.3 ± 4.7	53.4 ± 12.0	7.4 ± 1.1	0.26 ± 0.09	0.89 ± 0.15	6.4 ± 1.3	481.5 ± 12.2	48.8 ± 6.9	50.3 ± 5.4
AKR1B7	3.8 ± 2.9	44.0 ± 11.5	9.2 ± 0.9	9,200 ± 1,600	18,000 ± 2,800	9.0 ± 1.6	52.4 ± 1.2	ND	ND
AKR1C3	17.5 ± 10.0	3.9 ± 1.5	ND	ND	ND	9.1 ± 1.0	37.1 ± 1.3	ND	ND

Mean ± SD (n = 3–5). ND, not determined.

reductase inhibitors (ARI) with K_i values of 46–120 nM for the *p*-nitrobenzaldehyde reductase activities of AKR1B1 and AKR1B3, on the PGFS activity of AKR1B1, AKR1B3 and AKR1B7 (Table 1). Tolrestat was 6- and 3-fold more potent than sorbinil as inhibitor of the PGFS activity of AKR1B1 and AKR1B3, respectively (K_i values of 3.6 and 0.26 μM for tolrestat and 21.7 and 0.89 μM for sorbinil, respectively). However, both tolrestat and sorbinil only weakly inhibited the PGFS activity of AKR1B7, with a calculated K_i value of 9.2 and 18 mM, respectively. These results are in agreement with the report that the NADH-linked isocaproaldehyde reductase activity of AKR1B7 was insensitive to ARI (*21*).

Tolrestat inhibited the PGFS activity of AKR1B1 in a non-competitive manner, as demonstrated by the decrease in V_{max} without a change in K_m for PGH_2 (Fig. 4A). The inhibition profile of AKR1B1 by sorbinil

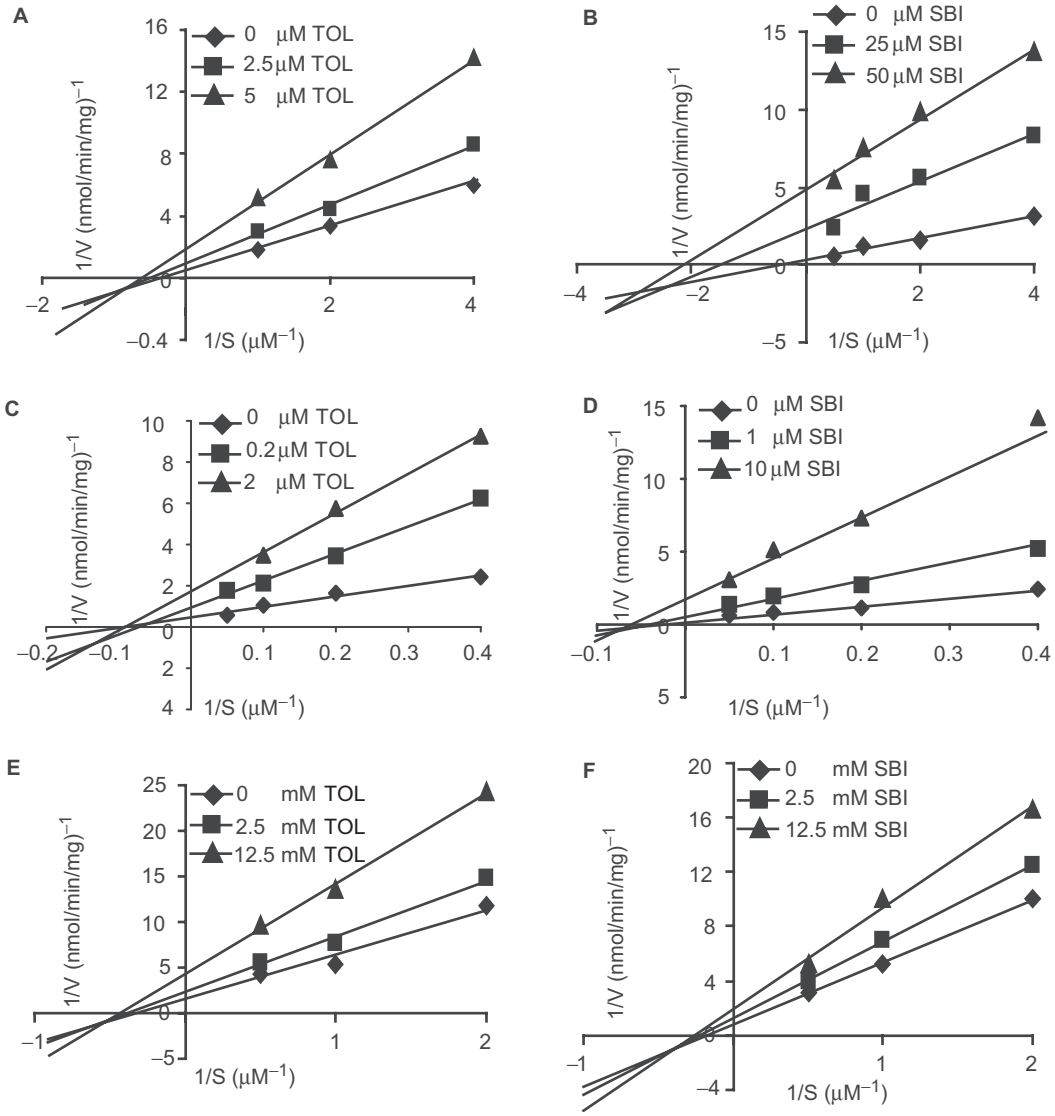

Fig. 4. **Lineweaver-Burk plots of the inhibition of PGFS activity of AKR1B proteins by tolrestat and sorbinil.** AKR1B proteins (A and B, AKR1B1; C and D, AKR1B3; and E and F, AKR1B7) were incubated with 1-[^{14}C] PGH_2 at 37°C for 2 min in the presence of various concentrations of tolrestat (A, C and E) or sorbinil (B, D and F). TOL, tolrestat; SBI, sorbinil.

was characterized as a mixed-type mechanism of inhibition, resulting in a decrease in V_{max} coupled to a decrease in K_m values (Fig. 4B). Tolrestat and sorbinil also inhibited the PGFS activity of both AKR1B3 (Fig. 4C and 4D, respectively) and AKR1B7 (Fig. 4E and 4F, respectively) in a non-competitive fashion. These results suggest that the substrate PGH_2 and ARI bound at different modes to these AKR1B enzymes.

DISCUSSION

Our data show that certain members of the AKR1B subfamily can now be considered as PGFS in human and mouse species. Members of the AKR1B subfamily are clearly different from each other in terms of their ability to produce $PGF_{2\alpha}$ from PGH_2. This PGFS activity could make them direct actors of cell signalling with potentially autocrine, paracrine or endocrine actions. This finding sheds new light on the way by which members of AKR1B sub-family modulate various physiological functions, e.g. renal filtration, reproduction, adipose tissue homeostasis or steroidogenesis, and could influence the onset of diabetic complications.

PGFS activity was detected in the canonical and widely expressed aldose reductases in different species e.g. human (AKR1B1), mouse (AKR1B3) (present data) and bovine (AKR1B5) (*13*). The mouse AKR1B7, a tissue-restricted ARLP also exhibited PGFS activity. These data imply that the mechanisms by which aldose reductases contribute to cellular protection in physiological conditions or to chronic tissue lesions in diabetic complications should be re-examined with respect to their PGFS activity (*10–12*). Indeed, ARI attenuated most hyperglycemia-induced osmotic and oxidative stress linked to the activation of the polyol pathway in diabetic

mice models (*23–27*) in diabetic patients (*28*, *29*) and in various types of cultured cells (*30–32*). However, as we have shown here, PGFS activity of AKR1B1 and AKR1B3 is sensitive to classical ARI, indicating that in the absence of selective inhibitors discriminating the different catalytic activities, it will be impossible to decipher the respective part of the polyol pathway activation, aldehyde detoxification and $PGF_{2\alpha}$ synthesis in the protective or deleterious functions of aldose reductases.

Although AKR1B7 was initially characterized as a mouse vas deferens androgen-dependent protein, its expression in the adrenal cortex and responsiveness to ACTH were two features conserved among rodents (*33*, *34*). In this steroidogenic gland, AKR1B7 was proposed to ensure the detoxification of isocaproaldehyde, a by-product of steroid biosynthesis (*22*). Interestingly, this function appeared to be taken in charge by AKR1B1 in human adrenocortical cells where its expression is also sensitive to ACTH/cAMP signalling pathway (*22*). These two proteins could share some regulating functions on endocrine activities in the adrenal gland through production of $PGF_{2\alpha}$. As the role of this prostanoid in adrenal physiology is completely unknown, this possibility remains a crucial question to address.

By contrast, in the adipose tissue, $PGF_{2\alpha}$ is a well known and potent inhibitor of adipocyte differentiation (*1*, *35*, *36*). Recently, we found that AKR1B7 was expressed in preadipocyte-enriched fractions obtained from peri-epididymal and peri-adrenal adipose tissues (*37*). In the same study, we also found that expression of AKR1B7 was down-regulated during the differentiation of adipose stromal cells in primary culture. Over-expression of AKR1B7 in 3T3 preadipocytes inhibited their differentiation to adipocytes, whereas its knock-down accelerated adipogenic differentiation by decreasing the production of $PGF_{2\alpha}$. Taken together with our present data, these observations support the possibility that the PGFS activity of AKR1B7 may be recruited to maintain a pool of pre-adipocytes and somehow repress the triggering of adipogenic differentiation.

Crystal structures of the complexes of AKR1B1 with ARI, such as sorbinil, tolrestat or zopolrestat, revealed that these inhibitors bind to the active site of AKR through their polar heads near the NADPH-binding site. In contrast, their hydrophobic moieties either bind to the native active site in the case of sorbinil or protrude into a pocket opened by conformational changes in the walls of the active site cleft and bind there in the case of tolrestat or zopolrestat (*38*). As tolrestat and sorbinil inhibited the PGFS activity of AKR1B1 and AKR1B3 with K_i values of 0.26–21.7 μM, resulting in non-competitive and mixed-type inhibition profiles, respectively, the ternary complex structures of AKR-NADPH-ARI and AKR-NADPH-PGH_2/$PGF_{2\alpha}$ analogues might be useful to determine the binding mode of PGH_2 to the catalytic site of these AKR enzymes. At last, the PGFS activity of AKR1B7 was remarkably resistant to inhibition by tolrestat and sorbinil (K_i = 9.2 and 18 mM, respectively), suggesting that mode of binding of PGH_2 and ARI to AKR1B7 was largely different from that in the case of AKR1B1 and AKR1B3.

ACKNOWLEDGEMENTS

We thank N. Uodome, Dr M. Lazarus and Dr B. K. Kubata, Osaka Bioscience Institute, for their assistance during the early stage of this research, Dr P. Val (CNRS UMR6247—GReD, France) for critical reading of the manuscript and M. Yamaguchi, M. Yamada and T. Nishimoto, Osaka Bioscience Institute, for secretarial assistance.

FUNDING

This work was supported in part by the Japan Society for the Promotion of Science Postdoctoral Fellowship (no. 02271 to Z.K.), Takeda Foundation (to M.M.), Fondation pour la Recherche Medicale (to S.L.) and Osaka City (to Y.U.).

CONFLICT OF INTEREST

None declared.

REFERENCES

1. Serrero, G., Lepak, N.M., and Goodrich, S.P. (1992) Prostaglandin F2 alpha inhibits the differentiation of adipocyte precursors in primary culture. *Biochem. Biophys. Res. Commun.* **183**, 438–442
2. Sasaki, S., Hozumi, Y., and Kondo, S. (2005) Influence of prostaglandin F2alpha and its analogues on hair regrowth and follicular melanogenesis in a murine model. *Exp. Dermatol.* **14**, 323–328
3. Watanabe, K. (2002) Prostaglandin F synthase. *Prostaglandins Other Lipid Mediat.* **68–69**, 401–407
4. Jez, J.M., Flynn, T.G., and Penning, T.M. (1997) A new nomenclature for the aldo-keto reductase superfamily. *Biochem. Pharmacol.* **54**, 639–647
5. Kuchinke, W., Barski, O., Watanabe, K., and Hayaishi, O. (1992) A lung type prostaglandin F synthase is expressed in bovine liver: cDNA sequence and expression in *E. coli*. *Biochem. Biophys. Res. Commun.* **183**, 1238–1246
6. Suzuki, T., Fujii, Y., Miyano, M., Chen, L.Y., Takahashi, T., and Watanabe, K. (1999) cDNA cloning, expression, and mutagenesis study of liver-type prostaglandin F synthase. *J. Biol. Chem.* **274**, 241–248
7. Suzuki-Yamamoto, T., Nishizawa, M., Fukui, M., Okuda-Ashitaka, E., Nakajima, T., Ito, S., and Watanabe, K. (1999) cDNA cloning, expression and characterization of human prostaglandin F synthase. *FEBS Lett.* **462**, 335–340
8. Kubata, B.K., Duszenko, M., Kabututu, Z., Rawer, M., Szallies, A., Fujimori, K., Inui, T., Nozaki, T., Yamashita, K., Horii, T., Urade, Y., and Hayaishi, O. (2000) Identification of a novel prostaglandin $F_{2\alpha}$ synthase in *Trypanosoma brucei*. *J. Exp. Med.* **192**, 1327–1338
9. Kabututu, Z., Martin, S.K., Nozaki, T., Kawazu, S., Okada, T., Munday, C. J., Duszenko, M., Lazarus, M., Thuita, L.W., Urade, Y., and Kubata, B.K. (2003) Prostaglandin production from arachidonic acid and evidence for a 9,11-endoperoxide prostaglandin H2 reductase in *Leishmania*. *Int. J. Parasitol.* **33**, 221–228
10. Yabe-Nishimura, C. (1998) Aldose reductase in glucose toxicity: a potential target for the prevention of diabetic complications. *Pharmacol. Rev.* **50**, 21–33
11. Spite, M., Baba, S.P., Ahmed, Y., Barski, O.A., Nijhawan, K., Petrash, J.M., Bhatnagar, A., and Srivastava, S. (2007) Substrate specificity and catalytic efficiency of aldo-keto reductases with phospholipid aldehydes. *Biochem. J.* **405**, 95–105

12. Srivastava, S.K., Ramana, K.V., and Bhatnagar, A. (2005) Role of aldose reductase and oxidative damage in diabetes and the consequent potential for therapeutic options. *Endocrinol. Rev.* **26**, 380–392
13. Madore, E., Harvey, N., Parent, J., Chapdelaine, P., Arosh, J.A., and Fortier, M.A. (2003) An aldose reductase with 20 alpha-hydroxysteroid dehydrogenase activity is most likely the enzyme responsible for the production of prostaglandin $F_{2\alpha}$ in the bovine endometrium. *J. Biol. Chem.* **278**, 11205–11212
14. Lau, E.T., Cao, D., Lin, C., Chung, S. K., and Chung, S.S. (1995) Tissue-specific expression of two aldose reductase-like genes in mice: abundant expression of mouse vas deferens protein and fibroblast growth factor-regulated protein in the adrenal gland. *Biochem. J.* **312 (Pt. 2)**, 609–615
15. Pailhoux, E.A., Martinez, A., Veyssiere, G.M., and Jean, C.G. (1990) Androgen-dependent protein from mouse vas deferens. cDNA cloning and protein homology with the aldo-keto reductase superfamily. *J. Biol. Chem.* **265**, 19932–19936
16. Taragnat, C., Berger, M., and Jean, C. (1988) Preliminary characterization, androgen-dependence and ontogeny of an abundant protein from mouse vas deferens. *J. Reprod. Fertil.* **83**, 835–842
17. Donohue, P.J., Alberts, G.F., Hampton, B.S., and Winkles, J.A. (1994) A delayed-early gene activated by fibroblast growth factor-1 encodes a protein related to aldose reductase. *J. Biol. Chem.* **269**, 8604–8609
18. Cao, D., Fan, S.T., and Chung, S.S. (1998) Identification and characterization of a novel human aldose reductase-like gene. *J. Biol. Chem.* **273**, 11429–11435
19. Hyndman, D.J. and Flynn, T.G. (1998) Sequence and expression levels in human tissues of a new member of the aldo-keto reductase family. *Biochim. Biophys. Acta* **1399**, 198–202
20. Komoto, J., Yamada, T., Watanabe, K., and Takusagawa, F. (2004) Crystal structure of human prostaglandin F synthase (AKR1C3). *Biochemistry* **43**, 2188–2198
21. Lefrancois-Martinez, A.M., Tournaire, C., Martinez, A., Berger, M., Daoudal, S., Tritsch, D., Veyssiere, G., and Jean, C. (1999) Product of side-chain cleavage of cholesterol, isocaproaldehyde, is an endogenous specific substrate of mouse vas deferens protein, an aldose reductase-like protein in adrenocortical cells. *J. Biol. Chem.* **274**, 32875–32880
22. Lefrancois-Martinez, A.M., Bertherat, J., Val, P., Tournaire, C., Gallo-Payet, N., Hyndman, D., Veyssiere, G., Bertagna, X., Jean, C., and Martinez, A. (2004) Decreased expression of cyclic adenosine monophosphate-regulated aldose reductase (AKR1B1) is associated with malignancy in human sporadic adrenocortical tumors. *J. Clin. Endocrinol. Metab.* **89**, 3010–3019
23. Ho, E.C., Lam, K.S., Chen, Y.S., Yip, J.C., Arvindakshan, M., Yamagishi, S., Yagihashi, S., Oates, P.J., Ellery, C.A., Chung, S.S., and Chung, S.K. (2006) Aldose reductase-deficient mice are protected from delayed motor nerve conduction velocity, increased c-Jun NH_2-terminal kinase activation, depletion of reduced glutathione, increased superoxide accumulation, and DNA damage. *Diabetes* **55**, 1946–1953
24. Lee, A.Y., Chung, S.K., and Chung, S.S. (1995) Demonstration that polyol accumulation is responsible for diabetic cataract by the use of transgenic mice expressing the aldose reductase gene in the lens. *Proc. Natl Acad. Sci. USA* **92**, 2780–2784
25. Song, Z., Fu, D.T., Chan, Y.S., Leung, S., Chung, S.S., and Chung, S.K. (2003) Transgenic mice overexpressing aldose reductase in Schwann cells show more severe nerve conduction velocity deficit and oxidative stress under hyperglycemic stress. *Mol. Cell Neurosci.* **23**, 638–647
26. Yagihashi, S., Yamagishi, S., Wada, R., Sugimoto, K., Baba, M., Wong, H.G., Fujimoto, J., Nishimura, C., and Kokai, Y. (1996) Galactosemic neuropathy in transgenic mice for human aldose reductase. *Diabetes* **45**, 56–59
27. Yagihashi, S., Yamagishi, S.I., Wada, R.R., Baba, M., Hohman, T.C., Yabe-Nishimura, C., and Kokai, Y. (2001) Neuropathy in diabetic mice overexpressing human aldose reductase and effects of aldose reductase inhibitor. *Brain* **124**, 2448–2458
28. Baynes, J.W. and Thorpe, S.R. (1999) Role of oxidative stress in diabetic complications: a new perspective on an old paradigm. *Diabetes* **48**, 1–9
29. Parry, G.J. (1999) Management of diabetic neuropathy. *Am. J. Med.* **107**, 27S–33S
30. Ramana, K.V., Friedrich, B., Srivastava, S., Bhatnagar, A., and Srivastava, S.K. (2004) Activation of nuclear factor-kappaB by hyperglycemia in vascular smooth muscle cells is regulated by aldose reductase. *Diabetes* **53**, 2910–2920
31. Ramana, K.V., Friedrich, B., Tammali, R., West, M.B., Bhatnagar, A., and Srivastava, S.K. (2005) Requirement of aldose reductase for the hyperglycemic activation of protein kinase C and formation of diacylglycerol in vascular smooth muscle cells. *Diabetes* **54**, 818–829
32. Srivastava, S., Ramana, K.V., Tammali, R., Srivastava, S.K., and Bhatnagar, A. (2006) Contribution of aldose reductase to diabetic hyperproliferation of vascular smooth muscle cells. *Diabetes* **55**, 901–910
33. Aigueperse, C., Martinez, A., Lefrancois-Martinez, A.M., Veyssiere, G., and Jean, C.I. (1999) Cyclic AMP regulates expression of the gene coding for a mouse vas deferens protein related to the aldo-keto reductase superfamily in human and murine adrenocortical cells. *J. Endocrinol.* **160**, 147–154
34. Val, P., Martinez, A., Sahut-Barnola, I., Jean, C., Veyssiere, G., and Lefrancois-Martinez, A.M. (2002) A 77-base pair LINE-like sequence elicits androgen-dependent mvdp/akr1-b7 expression in mouse vas deferens, but is dispensable for adrenal expression in rats. *Endocrinology* **143**, 3435–3448
35. Casimir, D.A., Miller, C.W., and Ntambi, J.M. (1996) Preadipocyte differentiation blocked by prostaglandin stimulation of prostanoid FP2 receptor in murine 3T3-L1 cells. *Differentiation* **60**, 203–210
36. Lepak, N.M. and Serrero, G. (1993) Inhibition of adipose differentiation by 9 alpha, 11 beta-prostaglandin F_2 alpha. *Prostaglandins* **46**, 511–517
37. Tirard, J., Gout, J., Lefrancois-Martinez, A.M., Martinez, A., Begeot, M., and Naville, D. (2007) A novel inhibitory protein in adipose tissue, the aldo-keto reductase AKR1B7: its role in adipogenesis. *Endocrinology* **148**, 1996–2005
38. Nakano, T. and Petrash, J.M. (1996) Kinetic and spectroscopic evidence for active site inhibition of human aldose reductase. *Biochemistry* **35**, 11196–11202